NUCL SCI TECH (2017) 28:170
https://doi.org/10.1007/s41365-017-0322-8

Water equivalence of some 3D dosimeters: a theoretical study based on the effective atomic number and effective fast neutron removal cross section

A. M. El-Khayatt[1,2]

Received: 4 October 2016 / Revised: 4 December 2016 / Accepted: 14 December 2016 / Published online: 15 November 2017

Abstract Effective atomic numbers for photon energy absorption ($Z_{PEA_{eff}}$) and their corresponding electron numbers ($N_{PEA_{eff}}$), and effective macroscopic removal cross sections of fast neutrons (Σ_R) were calculated for 27 different types of three-dimensional dosimeters, four types of phantom materials, and water. The values of $Z_{PEA_{eff}}$ and $N_{PEA_{eff}}$ were obtained using the direct method for energies ranging from 10 keV to 20 MeV. Results are presented relative to water, for direct comparison over the range of examined energies. The effect of monomers that are used in polymer gel dosimeters on the water equivalence is discussed. The relation between Σ_R and hydrogen content was studied. Micelle gel dosimeters are highly promising because our results demonstrate perfect matching between the effective atomic number, electron density number, and fast neutron attenuation coefficient of water.

Keywords 3D dosimeters · Water equivalence · Effective atomic number · Photon energy absorption · Removal cross section · Fast neutrons

✉ A. M. El-Khayatt
Ahmed_el_khayatt@yahoo.com; aelkhayatt@gmail.com

[1] Department of Physics, College of Science, Al Imam Mohammad Ibn Saud Islamic University (IMSIU), Riyadh 11432, Saudi Arabia

[2] Reactor Physics Department, NRC, Atomic Energy Authority, Cairo 13759, Egypt

1 Introduction

Modern radiation treatment techniques require three-dimensional (3D) dosimeters that can accurately measure dose distributions in three dimensions with high spatial resolution. The literature review suggests that 3D dosimeters are widely used in many radiotherapy applications, such as photon beam intensity-modulated radiation therapy (IMRT) [1], stereotactic radiosurgery (SRS), X-knife and γ-knife radiosurgery, and computed tomography-based (CT-based) brachytherapy, where steep dose gradients exist for conforming the prescription isodose to the target volume only [2]. In addition, developments in charged particle therapy allow radiation distributions to be tightly tailored to irregular 3D tumor volumes; as a result, 3D dosimeters are needed [3]. The need for 3D dose measurements is not limited to radiotherapy applications. Diagnostic radiology also requires measuring the distribution of radiation in patients undergoing medical imaging for a range of clinical diagnoses [4].

Two types of 3D dosimeters are commercially available: (1) gel dosimeters and (2) polyurethane radiochromic plastic dosimeters, which are known as "PRESAGE" dosimeters. Gel-based 3D dosimeters were first suggested in 1950 [5]. Gel dosimetry systems can in turn be divided into three types, based on: (1) the Fricke gel (featuring ferrous sulfate), (2) polymer gels, and (3) micelle gels. Micelle gel systems are a hybrid of PRESAGE and gel dosimeters.

The Fricke gel utilizes radiation-induced transformation of ferrous (Fe^{2+}) ions into ferric (Fe^{3+}) ions. This radiation-induced chemical change can be quantified by performing nuclear magnetic resonance (NMR) relaxation measurements [6] and can be used to obtain information on

the 3D spatial dose using magnetic resonance imaging (MRI) [7, 8]. Although the Fricke gel is easy to fabricate and handle, its post-irradiation stability is poor [9].

The first polymer dosimetry system was developed and reported by Alexander et al., in 1954 [10]. Polymer gels are chemical dosimeters based on dose-dependent radiation-induced polymerization and cross-linking of monomers in an irradiated volume. When a polymer gel is exposed to radiation, it becomes opaque via polymerization. Their optical density of these gels increases with increasing the absorbed dose, which is utilized by NMR [11] or optical CT [12]. Other, less established, readout techniques have been introduced, such as the X-ray CT [13], ultrasound tomography imaging [14], and vibrational spectroscopy [15].

Polymer gel dosimeters have several advantages, including tissue equivalence, high spatial resolution, and good post-irradiation stability. Polymer gels can be also potentially used for dosimetry in mixed neutron–gamma radiation fields [16, 17]. However, many polymer gel dosimeters have significant limitations and shortcomings; for example, they require external containers, which lead to edge artifacts, which in turn reduce the useful region of these dosimeters [18]. Many of these drawbacks were overcome following the development of plastic PRESAGE dosimeters [19]. This is an entirely new class of polymer dosimeters—radiochromic optically transparent 3D dosimeters based on polyurethane combined with leucodye leucomalachite green. Upon exposure to radiation, radiochromic material changes its color owing to the oxidation of leucodyes by halogen radicals [19].

PRESAGE has a number of potential advantages over both conventional polymer and Fricke gels. It is a transparent material with excellent properties for dosimetry, such as insensitivity of the dose response to oxygen and environmental conditions, a solid texture reducing edge effects by negating the need for an external container, and a radiochromic response that is well suited for accurate optical CT owing to the very low scattering fraction [20]. In addition, the polyurethane matrix prevents the diffusion of the dose distribution image [21]. Unfortunately, these dosimeters suffer from poor tissue equivalence and cannot be easily manufactured or molded into anthropomorphic phantoms [22].

Aiming to overcome the limitations of PRESAGE, Jordan and Avvakumov [23] and Babic et al. [24] developed radiochromic micelle gel dosimeters for optical readout. In their proposed approach, the color dye and halogen are dissolved in a gelatin gel. Because the color dye and halogen do not readily dissolve in the gelatin hydrogel, the dye and halogen are embedded in micelles [25]. A micelle gel changes its color upon irradiation [26]. These novel gel dosimeters have specific advantages compared with polyurethane dosimeters (such as PRESAGE dosimeters). The former exhibit better spatial stability and good water/soft tissue equivalence, over a wide range of photon energies. At the same time, the fabrication procedure of gelatin-based chemical dosimeters is less complicated than that of polyurethane-based dosimeters.

The 3D dosimeters evaluated in the present work can be divided into three main categories: (1) "conventional" (polymer and Fricke) gels, (2) "modern" (micelle) gels, and (3) polyurethane radiochromic plastic (PRESAGE) dosimeters. Conventional polymer gel dosimeters may be generally classified in terms of hypoxic, reduced toxic, or normoxic gels. Different types of hypoxic polymers have been suggested, such as polyacrylamide gelatin (PAG) [27] and bis-acrylamide nitrogen gelatin (BANG) gel formulations such as BANG-1. The term BANG is trademarked and a patent was acquired for this gel type [28]. BANG-2 uses acrylic acid as a monomer and NaOH to buffer the pH [29]. BANG gels have evolved to the third product from MGS research, known as BANG-3. The BANG-3 gel consists of BIS, methacrylic acid, sodium hydroxide, nitrogen, and gelatin. This new formulation exhibits stronger optical and NMR responses [8]. The monomers of these polymers are highly toxic; thus, they were replaced with reduced toxic monomers such as polyethylene glycol diacrylate bis-gelatin (PABIG) [30] and *N*-vinyl pyrrolidone argon (VIPAR) gels [31]. Even though these monomers are less toxic, all of these gel dosimeters have to be prepared under the hypoxic condition. Because these gel dosimeters are inhibited by oxygen, free oxygen has to be removed from the gel.

The term "normoxic" refers to a gel that can be fabricated under normal atmospheric conditions. In 2001, Fong et al. [32] developed the first normoxic gel dosimeter. This novel polymer gel dosimeter features a gel known as MAGIC, which is an acronym for the methacrylic acid, ascorbic acid, gelatin initiated by copper. The MAGIC gel utilizes the ascorbic acid oxygen scavenger, which binds free oxygen within the aqueous gelatin matrix into metallo-organic complexes, in a process that is initiated by copper sulfate. Replacing the ascorbic acid and copper sulfate by tetrakis in the MAGIC formulation yields a new formulation that consists of the methacrylic acid in gelatin and tetrakis (MAGAT) [33].

Gel manufacturers provided many types of such normoxic dosimeters, including MAGAS (which consists of the methacrylic acid and gelatin gel with ascorbic acid), HEAG (which consists of the hydroxy-ethyl-acrylate gel) [34], nPAG (which consists of the normoxic polyacrylamide gel), nMAG (which consists of the normoxic methacrylic gel) [35], and ABAGIC (which consists of the ascorbic acid, bis-acrylamide, in gelatin initiated by copper) [33].

In addition, some efforts were made to modify hypoxic gel dosimeters to normoxic ones. For example, the hypoxic PAG gel was combined with tetrakis (hydroxymethyl) phosphonium chloride (THPC) as an antioxidant, to form a normoxic gel dosimeter that utilizes the PAGAT gel (which consists of polyacrylamide, gelatin, and tetrakis phosphonium chloride) [36]. As another example, Senden et al. [37] replaced the highly toxic acrylamide monomer in the PAGAT gel with *N*-isopropylacrylamide, obtaining NIPAM. VIPAR polymer gel dosimeters were also modified, by Kantemiris et al. [38], to eliminate the need for deoxygenation in the manufacturing process. The new formulation, VIP, consists of *N*-vinyl pyrrolidone, gelatine, *N*,*N*′-methylenebisacrylamide, as well as of copper sulfate and ascorbic acid.

The effective atomic number, Z_{eff}, and the electron density, N_{eff}, are particularly valuable parameters for characterizing interactions in various multi-element materials. Many studies on Z_{eff} and N_{eff} of different materials for interactions of photons [39, 40], electrons [41], and heavy charged particles [42–44] are available. For a 3D dosimeter to be useful in radiation dosimetry, it should have water-equivalent radiological properties. The radiological properties such as the effective atomic number, Z_{eff}, effective electron density, N_{eff}, and mass density should ideally be the same as the radiological properties of water or tissue [45]. In a number of studies, a single Z_{eff} was calculated to support water equivalence of 3D dosimeters used in radiotherapy dosimetry (for an example, see [46]). In addition, energy-dependent data for the effective atomic number of photon interaction, $Z_{\text{PI}_{\text{eff}}}$, which is equivalent to taking into account the variation in the mass attenuation coefficient, μ/ρ, with photon energy, have been presented elsewhere for some 3D dosimeters [47]. On the other hand, only a few studies dealing with variations in the effective atomic number for photon energy absorption, $Z_{\text{PEA}_{\text{eff}}}$, which is equivalent to taking into account the variation in the mass energy absorption coefficient, μ_{en}/ρ, with photon energy, have been reported [48]. The dose is more strongly related to the mass absorption coefficient. It is therefore generally accepted that $Z_{\text{PEA}_{\text{eff}}}$ is more appropriate than $Z_{\text{PI}_{\text{eff}}}$ for water (or tissue) equivalence. This motivated us to conduct the studies described herein.

Attenuation of fast neutrons by hydrogenous materials may be approximately calculated using the empirical Albert–Welton kernel and removal cross sections [49]. The macroscopic effective cross section for removal of fast neutrons, for simplicity referred to as removal cross section, Σ_{R} (cm^{-1}), is the probability that a fast or fission-energy neutron undergoes one collision that removes it from the group of penetrating, non-collided neutrons [50]. Here, attenuation or "removal" implies removal from the group of fast neutrons. Because 3D dosimeters in general have sufficient hydrogen content, they can be considered as ideal substances for application of the removal cross-sectional concept. Moreover, fast neutrons are used for treating certain types of cancer. These particles are also likely to be advantageous over other particles that are used in radiation therapy, such as photons, electrons, and protons, owing to their high linear energy transfer (LET) radiation and because damage is inflicted primarily by nuclear interactions [51]. However, to the best of the author's knowledge, no reports have been published regarding water equivalence of 3D dosimeters with respect to the attenuation of fast neutrons based on the concept of removal cross section.

In this study, water equivalence of 3D dosimeters is discussed from the point of view of photon energy absorption and fast neutron attenuation coefficient. The calculated values of effective atomic numbers for photon energy absorption, $Z_{\text{PEA}_{\text{eff}}}$, over a wide range of energies (10 keV–20 MeV) as well as the removal cross sections of fast neutrons, Σ_{R}, were considered for 27 different types of 3D dosimeters. For comparison, these parameters were also evaluated for water, soft tissue, brain tissue, muscle, and bone.

2 Materials and methods

Table 1 lists the elemental compositions, expressed as percentage by mass, of the 3D polymers and micelle gels that were considered in this study.

Table 3 lists the chemical formulae and fractional weights of six PRESAGE formulations that were studied here. Excluding PRESAGE6, which does not contain any halogens, the other formulations have different halogen contents. PRESAGE formulations 3–6 contain very small concentrations ($\leq$ 0.03 wt.%) of metal compounds. Metal compounds accelerate the polymerization process, improve the post-irradiation response stability, and yield good sensitivity to radiation [52].

The Fricke gel dosimeter and some phantom materials are listed in Table 2. The bone, muscle, and tissue definitions used data that were obtained from the international commission of radiation units and measurements (ICRU) [53].

2.1 Calculations of the effective atomic number, Z_{eff}, and effective electron density, N_{eff}, over a wide range of energies

In composite materials, for photon interactions, the atomic number cannot be represented uniquely across the entire range of energies, as in the case of elements, by a

Table 1 Elemental compositions and fractional weights % (w_e) of different 3D polymers and micelle gels

Abbreviation or acronym	Meaning	w_H	w_C	w_N	w_O	w_{Na}	w_P	w_S	w_{Cl}	w_{Cu}
Hypoxic										
PAG	Polyacrylamide gel	10.7367	6.2009	2.1804	80.8820			1.54E−4		5.06E−4
BANG-1	BIS, acrylamide, nitrogen, and gelatin	10.7685	5.6936	2.0063	81.5316					
BANG-2	Refers to successor of BANG-1	10.6369	5.6728	1.4152	81.7004	0.5748				
BANG-3[a]	Refers to successor of BANG-2	10.5100	5.6400	1.3500	81.7300	0.5800				
Reduced toxic										
VIPAR	n-Vinyl pyrrolidone argon	10.7321	7.1825	2.0638	80.0217					
PABIG	Polyethylene glycol diacrylate bis-gelatin	10.6454	6.8373	1.5649	80.9524					
Normoxic										
MAGIC	Methacrylic ascorbic acid in gelatin initiated by copper	10.5473	9.2231	1.3916	78.8373			3.00E−4		5.00E−4
MAGAS	Methacrylic acid gelatin with ascorbic acid	10.5087	9.3591	1.3799	78.7523					
ABAGIC	Ascorbic acid, bis-acrylamide, in gelatin initiated by copper	10.5263	8.963	3.105	77.4054			3.00E−4		5.00E−4
MAGAT	Methacrylic acid, gelatin, and tetrakis	10.522	9.5417	1.366	77.6988		0.4064		0.4651	
PAGAT	Polyacrylamide gel and tetrakis	10.7257	6.2174	1.9688	80.2166		0.4064		0.4651	
VIP[b]	Refers to normoxic formulation of VIPAR	10.4521	11.6534	2.9215	74.9725					
nPAG	Normoxic polyacrylamide gel	10.7107	6.5251	2.1814	80.1385		0.5748		0.2371	
nMAG	Normoxic methacrylic acid-based gel	10.6775	7.5066	1.3868	80.2527		0.0822		0.0941	
NIPAM1[c]	*N*-Isopropylacrylamide	10.8055	6.5998	1.7531	79.9702		0.4064		0.4651	
NIPAM2[d]	*N*-Isopropylacrylamide	10.6400	13.6400	3.1660	72.2300		0.1534		0.1756	
NIPAM3[d]	*N*-Isopropylacrylamide	11.1700	29.9400	3.2820	55.2800		0.1534		0.1756	
HEAG	Hydroxy-ethyl-acrylate gel	10.7641	5.7243	1.4152	82.0964					
Micelle[e]										
MGDF1	Refers to micelle gel dosimeter formulation 1	11.0400	2.2900	0.0100	86.4900				0.1700	
MGDF2	Refers to micelle gel dosimeter formulation 2	10.8700	3.7900	0.0100	84.1400	0.1600		0.1100	0.9100	

[a]Ref. [16]
[b]Ref. [38]
[c]Ref. [37]
[d]Ref. [26]
[e]Ref. [61]

single number. The procedure for calculating the effective atomic number using the direct method has been described elsewhere [54]. The effective atomic numbers of the studied samples were calculated using the following practical formula [55]:

$$Z_{\mathrm{PEA_{eff}}} = N_{\mathrm{A}} \frac{\sum_i f_i A_i \left(\frac{\mu_{\mathrm{en}}}{\rho}\right)_i}{\sum_i f_i \frac{A_i}{Z_i} \left(\frac{\mu_{\mathrm{en}}}{\rho}\right)_i}, \quad (1)$$

where N_A is the Avogadro constant and f_i is the molar fraction of the ith constituent element (normalized, so that $\Sigma_i f_i = 1$). Here, μ_{en}/ρ is the mass energy absorption coefficient, which was obtained from the tabulation of Hubbell and Seltzer [56]. Each material was considered to be a mixture of different compounds in various proportions (Tables 1, 2, 3).

Table 2 Elemental compositions and fractional weights % (w_e) of water and different 3D Fricke gel dosimeters

Material	w_H	w_C	w_N	w_O	w_{Na}	w_{Mg}	w_P	w_S	w_{Cl}	w_K	w_{Ca}	w_{Fe}	w_{Cu}	w_{Zn}
Fricke phantom[a]	10.736	2	0.67	85.736	0.0021			0.85	0.0033			0.0026		
Bone (cortical)	4.7234	14.4330	4.1990	44.6096		0.2200	10.4970	0.3150			20.9930			0.0100
Tissue (soft)	10.2000	14.3000	3.4000	70.8000	0.2000		0.3000	0.3000	0.2000	0.3000				
Muscle (striated)	11.000	12.3000	3.5000	72.900	0.0800	0.0200	0.2000	0.3000						
Water	11.1898			88.8102										

[a]Ref. [53]

Table 3 Relevant molecular formulae, elemental compositions, and fractional weights % (w_e) of the PRESAGE formulations used in this study

Material	Formula	w_H	w_C	w_N	w_O	w_S	w_{Cl}	w_{Zn}	w_{Br}	w_{Sn}
PRESAGE1[a]	$C_{1758}N_{121}H_{3000}O_{442}S_4Cl_{30}Br_1$	8.8474	61.7815	4.9589	20.6912	0.3753	3.1119		0.2338	
PRESAGE2[b]	$C_{481}H_{842}N_{30}O_{129}Cl_9Br_1$	8.925	60.7555	4.419	21.7048		3.3555		0.8403	
PRESAGE3[c]	$C_{64951}N_{4391}H_{113401}O_{15791}C_{11414}Sn_1$	9.08	61.9725	4.8858	20.07		3.9823			0.0094
PRESAGE4[c]	C_{35904} N_{2426} $H_{62685}O_{8728}C_{1819}Zn_1$	9.063	61.858	4.8742	20.0305		4.1649	0.0094		
PRESAGE5[c]	$C_{50455}N_{3417}H_{88064}O_{12295}C_{1775}Br_{17}Sn_1$	9.1669	62.5851	4.9428	20.3152		2.8375		0.1403	0.0123
PRESAGE6[d]	$C_{18746}N_{1239}H_{32825}O_{4455}C_{360}Sn_1$	9.4176	65.3203	4.9398	20.2885					0.0338

[a]Ref. [25]

[b]Ref. [22]

[c]Ref. [52]

[d]Ref. [60]

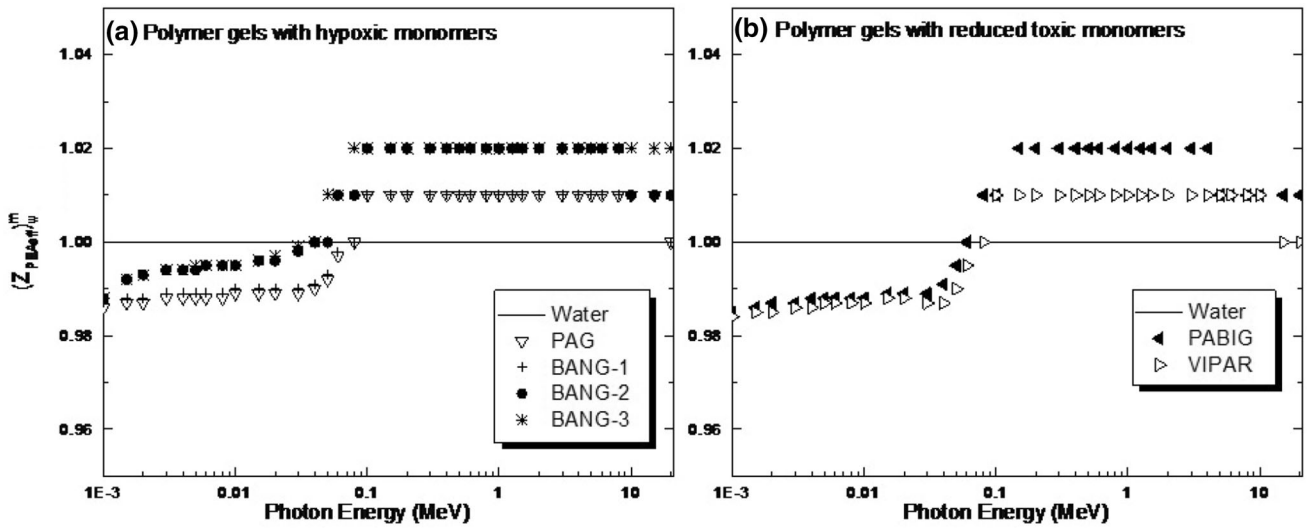

Fig. 1 $(Z_{PEA_{eff}})^m_w$: the ratios of $Z_{PEA_{eff}}$ values of **a** hypoxic and **b** reduced toxic monomers of 3D polymer gel dosimeters to those of water, as a function of energy

The effective electron density, $N_{PEA_{eff}}$, expressed in the number of electrons per unit mass, is closely related to the effective atomic number, and is given by

$$N_{PEA_{eff}} = N_A \frac{nZ_{PEA_{eff}}}{\sum_i n_i A_i} = N_A \frac{Z_{PEA_{eff}}}{\langle A \rangle} \text{(electrons/g)}, \quad (2)$$

where $\langle A \rangle$ is the mean atomic mass, which is given by

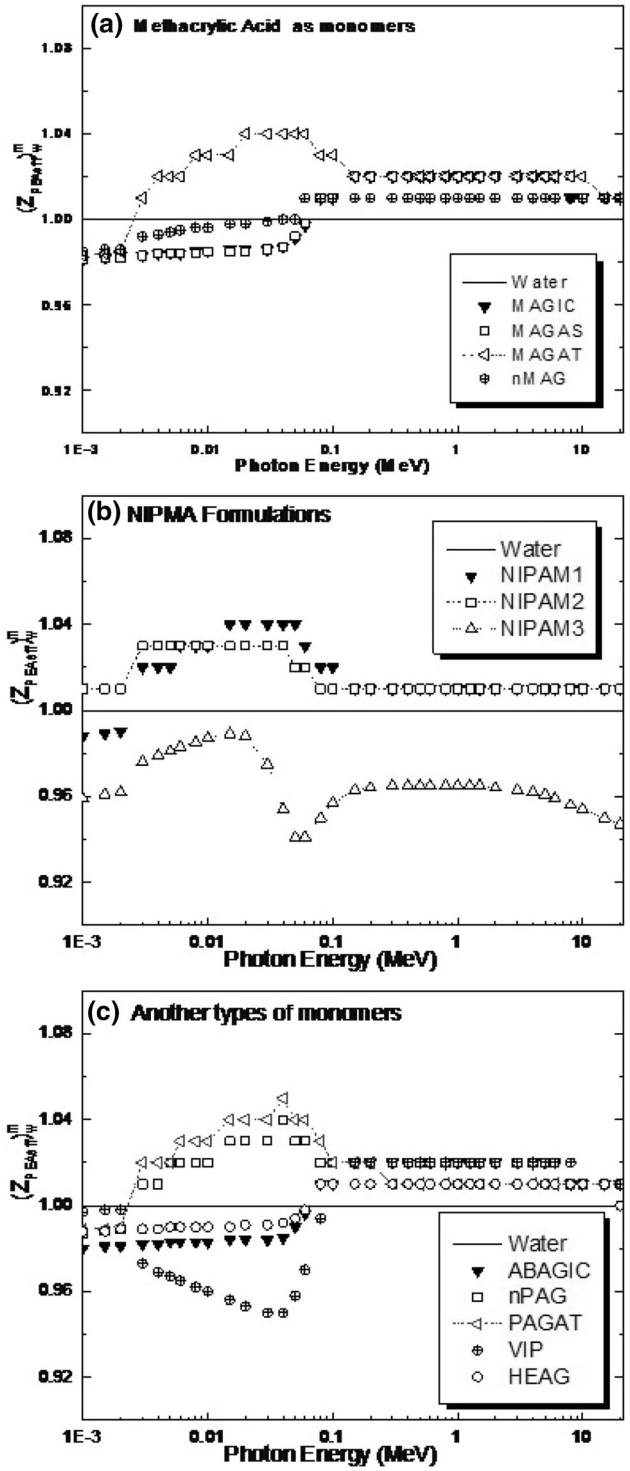

Fig. 2 $(Z_{PEA_{eff}})^{m}_{w}$: the ratios of $Z_{PEA_{eff}}$ for different types of normoxic 3D polymer gel dosimeters **a** methacrylic acid monomers, **b** NIPAM formulations, and **c** other monomers, to those of water, as a function of energy

$$\langle A \rangle = \sum_i f_i A_i, \tag{3}$$

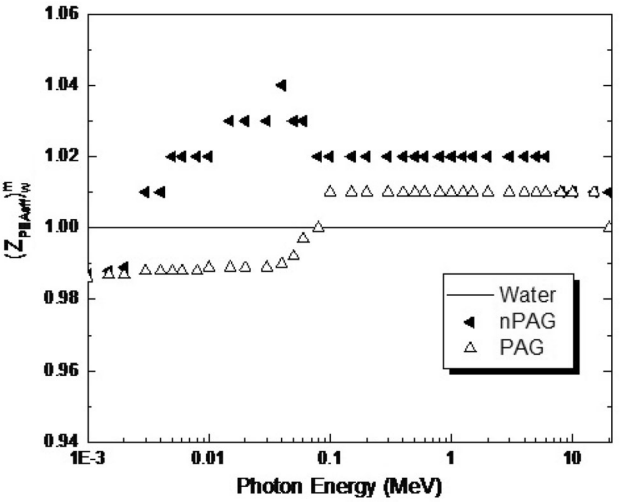

Fig. 3 $(Z_{PEA_{eff}})^{m}_{w}$: the ratios of $Z_{PEA_{eff}}$ for the hypoxic PAG 3D dosimeter and its normoxic formulation, nPAG, to those of water, as a function of energy

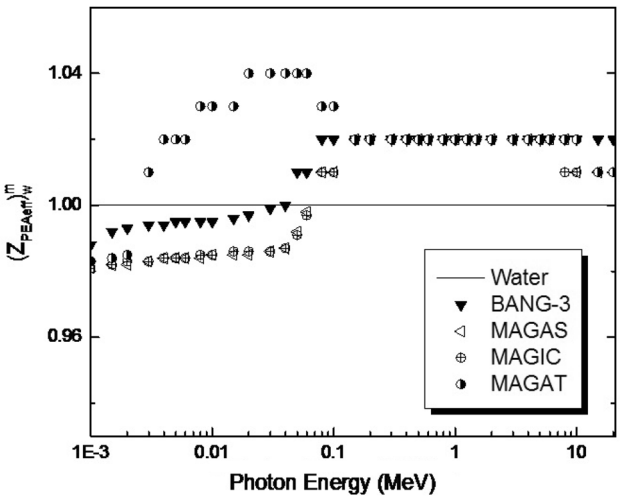

Fig. 4 $(Z_{PEA_{eff}})^{m}_{w}$: the ratios of $Z_{PEA_{eff}}$ for the hypoxic BANG-3 3D dosimeter and normoxic formulations that have the same monomers (methacrylic acid), to those of water, as a function of energy

where A_i is the atomic mass.

The effective atomic numbers and effective electron densities for photon energy absorption as a function of photon energy (for energies ranging from 10 keV to 20 MeV) were calculated for 27 3D dosimeters, four biological materials, and water.

2.2 Calculation of the effective macroscopic cross section for removal of fast neutrons, Σ_R

The concept of the removal cross section is valid for fast neutrons with energies in the 2–12 MeV range, because in this range the removal cross section is considered to be

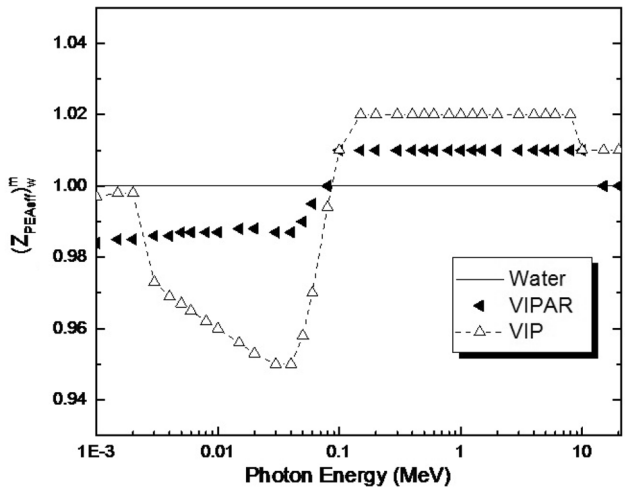

Fig. 5 $(Z_{PEA_{eff}})^{m}_{w}$: the ratios of $Z_{PEA_{eff}}$ for the reduced toxic VIPAR 3D dosimeter and its normoxic formulation, VIP, to those of water, as a function of energy

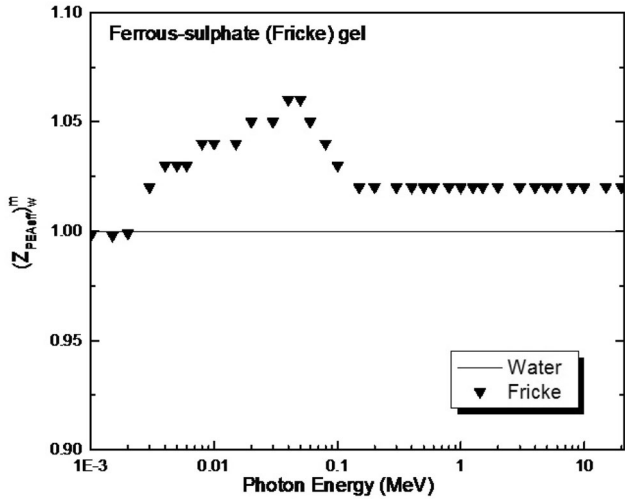

Fig. 6 $(Z_{PEA_{eff}})^{m}_{w}$: the ratios of $Z_{PEA_{eff}}$ for the Fricke gel 3D dosimeter, to those of water, as a function of energy

nearly constant [57]. The method assumes that collisions with hydrogen atoms are equivalent to absorption events.

The removal cross section for a given compound may be calculated from the value of Σ_R or Σ_R/ρ for various elements in the compound or mixture, using the mixture rule [57]:

$$\Sigma_R = \sum_i \rho_i (\Sigma_R/\rho)_i, \quad (4)$$

where ρ_i and $(\Sigma_R/\rho)_i$ are the partial density (the density as it appears in the mixture) and mass removal cross section of the ith constituent, respectively.

The NXcom computer program [50] was employed for calculating the effective removal cross sections for the studied 3D dosimeters, water, and phantom materials.

3 Results and discussion

3.1 Energy dependence of $(Z_{PEA_{eff}})^{m}_{w}$ and $(N_{PEA_{eff}})^{m}_{w}$ ratios

To evaluate the degree of water equivalence, we have calculated, for each material, the ratio, $(Z_{PEA_{eff}})^{m}_{w}$, of $(Z_{PEA_{eff}})_{m}$ (characterizing the material) to $(Z_{PEA_{eff}})_{w}$ (characterizing water), over the full range of energies (from 1 keV to 20 MeV). These ratios, $(Z_{PEA_{eff}})^{m}_{w}$, are plotted in Figs. 1, 2, 3, 4, 5, 6, 7, 8 and 9. The effective electron density N_{PEAeff} is closely related to the effective atomic number, as shown by Eq. 2. Consequently, the energy dependence of $(N_{PEA_{eff}})^{m}_{w}$ is similar to that of $(Z_{PEA_{eff}})^{m}_{w}$. Therefore, only one example for the variation in $(N_{PEA_{eff}})^{m}_{w}$ with photon energy is given in Fig. 7b.

3.1.1 Water equivalence of conventional and modern gels

Figure 1 shows the $(Z_{PEA_{eff}})^{m}_{w}$ ratio curves for some 3D polymer gel dosimeters based on hypoxic and reduced toxic monomers for photon energy absorption, as it varies with photon energy. Because all polymer dosimeters contain water as the major constituent, they exhibit similar variations with energy; in most cases, these curves differ from that for water by no more than 2% (Fig. 1).

Considering the mean disparity, the effective atomic number for the photon energy absorption of BANG-1 (as an example of an hypoxic polymer) is most similar to that of water, as shown in Fig. 1a, with no constituents with $Z > 8$. The results for the VIPAR formulation, shown in Fig. 1b, also closely match those for water.

As for normoxic gels based on the methacrylic acid as monomers (Fig. 2a), nMAG is the most similar to water in terms of $Z_{PEA_{eff}}$, as shown in Fig. 2a. Moreover, it was shown that replacing the ascorbic acid by tetrakis, as in MAGAT, makes the $Z_{PEA_{eff}}$ matching less tight.

For NIPMA normoxic formulations, Fig. 2b shows that for NIPAM 3, the gel that matches water the least, the $Z_{PEA_{eff}}$ values are systematically lower than those for water, especially for photon energies above 400 keV. The low matching may be attributed to the lower oxygen content compared with water.

On the other hand, Fig. 2c shows that $(Z_{PEA_{eff}})^{m}_{w}$ change with energy for some other normoxic gel dosimeters that are based on other monomer types. The results in this figure suggest that the formulations based on hydroxyethyl-acrylate (HEAG) and bis-acrylamide (ABAGIC) monomers are the most similar to water.

The ratios $(Z_{PEA_{eff}})^{m}_{w}$ for the hypoxic PAG dosimeter and its normoxic formulation, nPAG, are plotted in Fig. 3. A better similarity to water is observed for the hypoxic

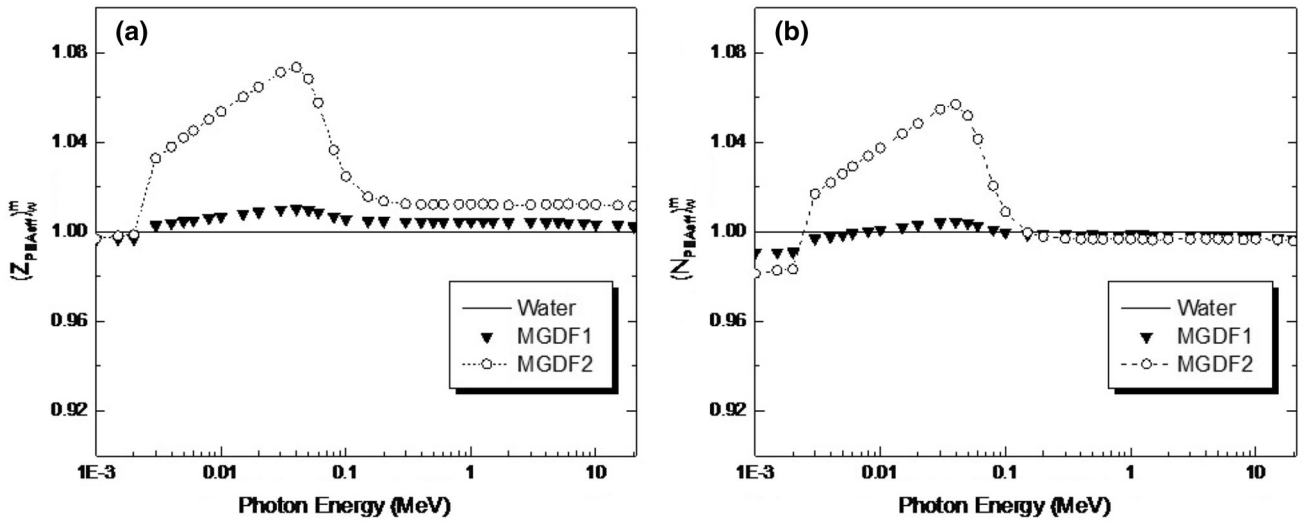

Fig. 7 $(Z_{PEA_{eff}})^{m}_{w}$ and $(N_{PEA_{eff}})^{m}_{w}$: the ratios of **a** $Z_{PEA_{eff}}$ and **b** their corresponding $N_{PEA_{eff}}$ values, for two formulations of micelle gel 3D dosimeters, to those of water, as a function of energy

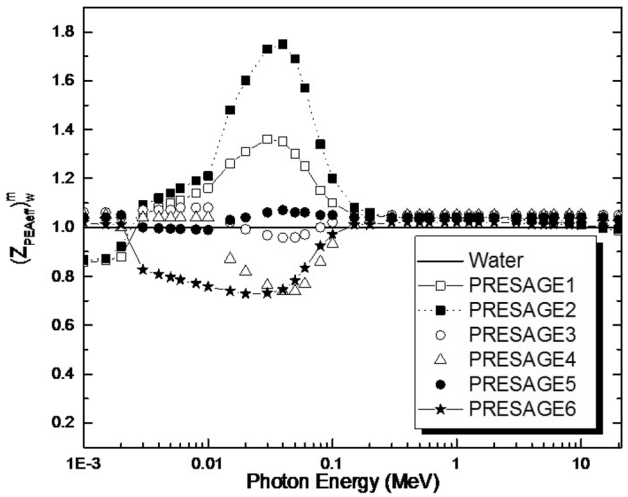

Fig. 8 $(Z_{PEA_{eff}})^{m}_{w}$: the ratios of $Z_{PEA_{eff}}$ for different PRESAGE formulations of 3D dosimeters, to those of water, as a function of energy

formulation compared with its normoxic gel, throughout the entire range of energies. Similar behaviors were observed for the hypoxic BANG-3 gel that is based on the methacrylic acid as a monomer and those normoxic gels that are based on the same monomer (methacrylic acid with an oxygen scavenger), as shown in Fig. 4.

Finally, Fig. 5 shows the ratios $(Z_{PEA_{eff}})^{m}_{w}$ for the reduced toxic VIPAR and its normoxic formulation, VIP. The results indicate that the reduced toxic formulation matches water better than its normoxic edition.

The results in Fig. 6 suggest that the $Z_{PEA_{eff}}$ values for the Fricke gel are systematically higher than that of water, especially at low energies. Nevertheless, for energies above 100 keV, the results for the Fricke gel dosimeter were in close agreement (2%) with those for water.

The $(Z_{PEA_{eff}})^{m}_{w}$ curves for two micelle formulations are shown in Fig. 7. The MGDF1 formulation exhibits a perfect match to the effective atomic and electron density numbers of water.

3.1.2 Water equivalence of PRESAGE dosimeters

The $(Z_{PEA_{eff}})^{m}_{w}$ ratio curves for PRESAGE dosimeters (Fig. 8) show a maximal difference at $\sim$ 35 keV, indicating that the effective atomic numbers differ from that of water by factors as large as 1.76 (PRESAGE2) and 1.37 (PRESAGE1) and as small as 0.74 (PRESAGE4 and PRESAGE6). However, all PRESAGE formulations come close to matching water for energies higher than 100 keV. Moreover, PRESAGE3 and PRESAGE5 formulations exhibit good matching for the entire range of energies, with the corresponding maximal differences, at low energies, being under 6%.

Conventional and modern gels and PRESAGE dosimeters typically match water better than water matches some tissues (Fig. 9b), and in most cases, slight differences in effective atomic number between water and dosimeters may be considered insignificant, especially over the therapeutic range of energies, 1–20 MeV.

3.2 Effective mass removal cross section of fast neutrons, Σ_R/ρ

Figure 10 shows the ratios, $(\Sigma_R)^{m}_{w}$, of Σ_R for the various 3D dosimeters, to Σ_R of water. Because all dosimetric materials are predominantly composed of water, the results

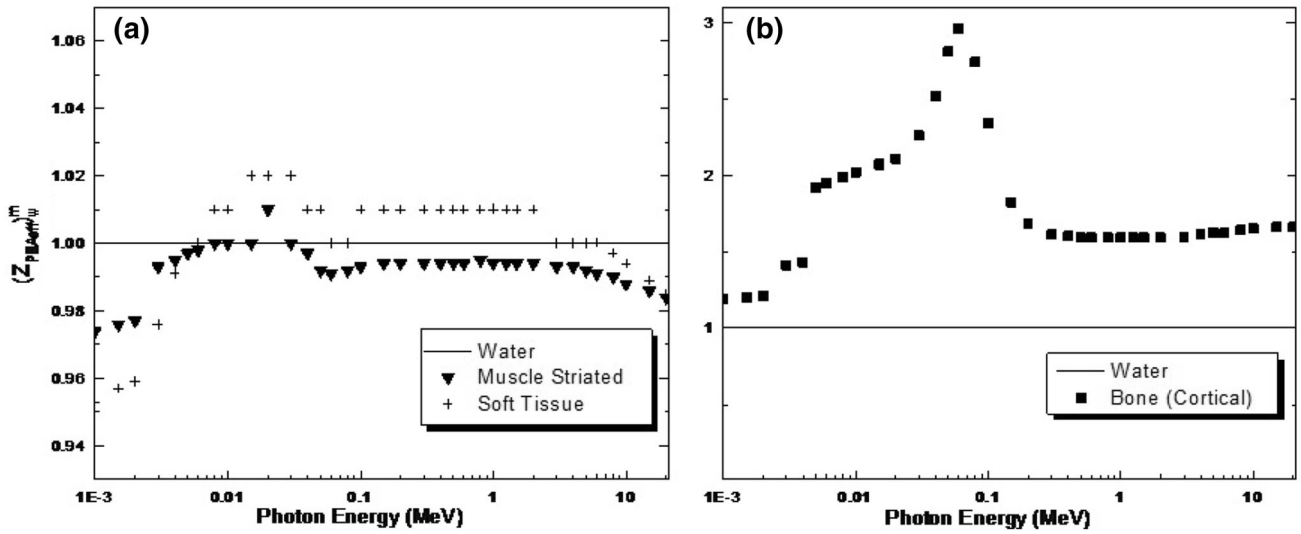

Fig. 9 $(Z_{PEA_{eff}})^{m}_{w}$: the ratios of $Z_{PEA_{eff}}$ for some phantom materials such as **a** muscle and soft tissue and **b** bone, to those of water, as a function of energy

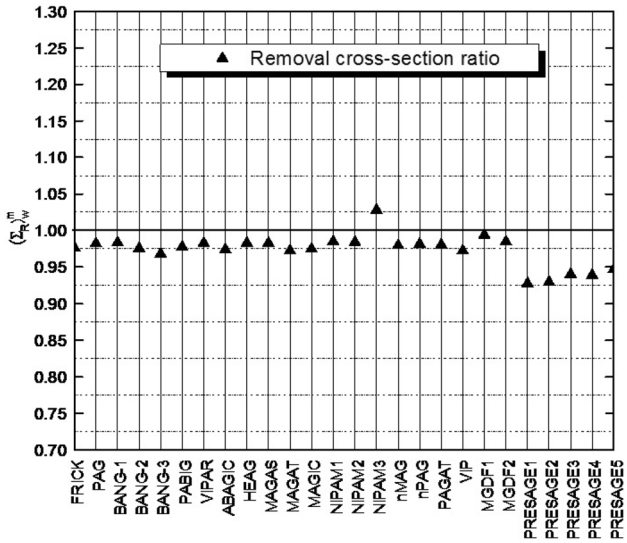

Fig. 10 $(\Sigma_R)^{m}_{w}$: the ratios of Σ_R for various types of 3D dosimeters, to those of water

show that, except for PRESAGE formulations, the removal cross sections of fast neutrons of 3D dosimeters and water agree well (1.5–3%). Owing to their low hydrogen and oxygen concentrations, differences ($\sim$ 7.5%) from the values for water were observed for PRESAGE1 and PRESAGE2. Excluding the NIPMA3 formulation, all 3D dosimeter materials had lower Σ_R values compared with water. It is also obvious that the considered micelle gel dosimeters exhibit excellent matching to water.

Table 4 lists the calculated values of Σ_R for the studied materials. Table 4 and Fig. 11 show that the removal cross-sectional values for all phantom materials are quite close ($\sim \pm$ 1.5%) to that of water—except the bone tissue, which varied by $\sim$ 38%, which was owing to a lower hydrogen content.

Considering the values of $(\Sigma_R)^{m}_{w}$, the 3D dosimetric materials were found to match water better than water matches some tissues (as indicated in Fig. 11 and Table 4).

As mentioned above, the concept of the removal cross section is based on the presence of hydrogen. Therefore, Figs. 12 and 13 show the variation of the removal cross section of fast neutrons with the hydrogen content. The results presented in these figures show that Σ_R systematically increases with increasing the dosimetric material's hydrogen content (w_H). In addition, it has been found that the variation for most polymer gel dosimeters and different PRESAGE formulations can be captured by a simple linear regression equation, with excellent correlation coefficient R^2, as shown in Figs. 12 and 13, respectively.

3.3 Accuracy of calculations

Equation 1 prescribes that the accuracy of the effective atomic number calculation is basically determined by the accuracy of the elemental mass attenuation coefficient $(\mu/\rho)_i$. For energies in the range of interest to medical and biological applications, from 5 keV to a few MeV, Hubbell showed that the uncertainty of $(\mu/\rho)_i$ is on the order of 1–2%. Discrepancies, between experimental results and theoretical calculations, of 25–50%, are known to occur for low energies, in the 1–4 keV range [58]. Therefore, our calculated Z_{eff} values are accurate to within a few percent, for energies above 5 keV. On the other hand, the values of Σ_R that were obtained from Eq. 4 are usually accurate to within $\sim$ 10% of the corresponding experimentally determined values [59].

Table 4 Hydrogen content (weight fraction), calculated Σ_R, and $(\Sigma_R)_w^m$ ratios for Σ_R, for various studied materials, to those of water

Material	w_H	Σ_R	$(\Sigma_R)_w^m$
Water	0.11190	0.10288	1.000
FRICKE	0.00107	0.10047	0.977
PAG	0.10737	0.10105	0.982
BANG-1	0.10769	0.10117	0.983
BANG-2	0.10637	0.10038	0.976
BANG-3	0.10510	0.09958	0.968
PABIG	0.10645	0.10058	0.978
VIPAR	0.10732	0.10112	0.983
ABAGIC	0.10526	0.10019	0.974
HEAG	0.10764	0.10113	0.983
MAGAS	0.10509	0.10113	0.983
MAGAT	0.10522	0.10002	0.972
MAGIC	0.10547	0.10026	0.974
NIPAM1	0.10806	0.10134	0.985
NIPAM2	0.10640	0.10123	0.984
NIPAM3	0.11170	0.10577	1.028
nMAG	0.10678	0.10079	0.980
nPAG	0.10711	0.10098	0.982
PAGAT	0.10726	0.10086	0.980
VIP	0.10452	0.10003	0.972
MGDF1	0.11040	0.10224	0.994
MGDF2	0.10870	0.10130	0.985
PRESAGE1	0.08847	0.09545	0.928
PRESAGE2	0.08925	0.09563	0.929
PRESAGE3	0.09080	0.09673	0.940
PRESAGE4	0.09063	0.09660	0.939
PRESAGE5	0.09167	0.09742	0.947
PRESAGE6	0.09418	0.09954	0.968
Bone (cortical)	0.047234	0.06367	0.619
Brain tissue	0.10700	0.10147	0.986
Tissue (soft)	0.10200	0.10466	1.017
Muscle (striated)	0.10997	0.10320	1.003

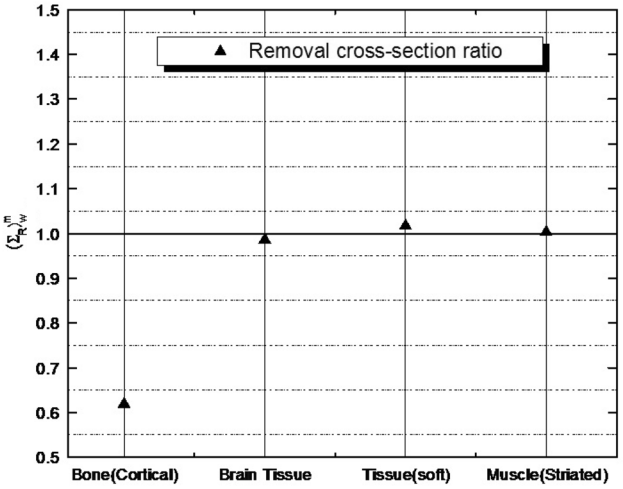

Fig. 11 $(\Sigma_R)_w^m$: the ratios of Σ_R for some phantom materials, to those of water

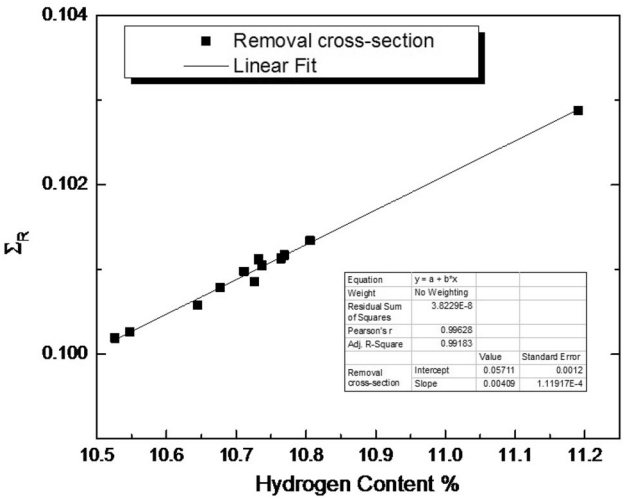

Fig. 12 Removal cross section of fast neutrons for some polymer gel 3D dosimeters, as a function of hydrogen content

4 Conclusion

Here, we have presented effective atomic numbers and effective electron densities for photon energy absorption as well as the removal cross sections for 31 dosimetric and phantom materials. The results are presented relative to water, to allow direct comparisons over a range of energies. Regarding the mean disparity over a wider range of energies, our results suggest, broadly, that highly toxic and reduced toxic polymer gels typically match water better than water matches normoxic gels, and replacing the ascorbic acid by tetrakis yields worse matching. More specifically, the results show that the 3D dosimeters that exhibit the closest radiological water equivalence are PAG, VIPAR, nMAG, NIPAM2, HEAG, PRESAGE3, PRESAGE5, and MGDF1 formulations. PRESAGE1 and PRESAG2, Fricke and NIPAM3 dosimeters, on the other hand, were found to be the least water equivalent over all energies.

With regard to the removal cross sections, which were calculated here for the first time, it was found that the MGDF1 micelle gel, conventional (polymer and Fricke) gels and PRESAGE formulations typically very closely, closely, and considerably match the values for water, respectively. Differences in Σ_R between water and dosimeters were attributed to hydrogen content. Moreover, simple linear dependences between the hydrogen content (w_H) and Σ_R were demonstrated.

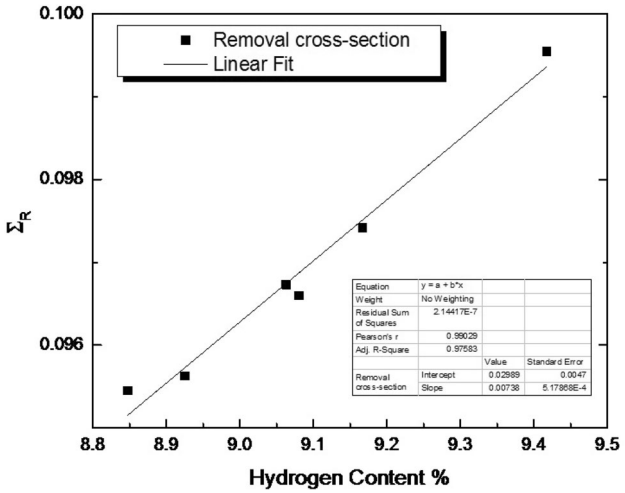

Fig. 13 Removal cross section of fast neutrons for PRESAGE formulation 3D dosimeters, as a function of hydrogen content

References

1. K. Vergote, Y. De Deene, F. Claus et al., Application of monomer/polymer gel dosimetry to study the effects of tissue inhomogeneities on intensity-modulated radiation therapy (IMRT) dose distributions. Radiother. Oncol. **67**, 119–128 (2003). https://doi.org/10.1016/S0167-8140(02)00376-6
2. J.V. Dyk, *The Modern Technology of Radiation Oncology* (Medical Physics Publishing, Madison, 1999), pp. 313–348
3. C. Greco, S. Wolden, Current status of radiotherapy with proton and light ion beams. Cancer **109**, 1227–1238 (2007). https://doi.org/10.1002/cncr.22542
4. J.T. Busberg, J.A. Siebert, E.M. Leidholdt et al., *The Essential Physics of Medical Imaging*, 3rd edn. (Lippincott, Williams and Wilkins, Baltimore, 2012); ISBN: 9780781780575
5. M.J. Day, G. Stein, Chemical effects of ionizing radiation in some gels. Nature **166**, 146–147 (1950). https://doi.org/10.1038/166146a0
6. J.C. Gore, Y.S. Kang, R.J. Schulz, Measurement of radiation dose distributions by nuclear magnetic resonance (NMR) imaging. Phys. Med. Biol. **29**, 1189–1197 (1984). https://doi.org/10.1088/0031-9155/29/10/002
7. A. Appleby, E.A. Christman, V. Leghrouz, Imaging of spatial radiation dose distribution in agarose gels using magnetic resonance. Med. Phys. **14**, 382–384 (1987). https://doi.org/10.1118/1.596052
8. M. Oldham, J.H. Siewerdsen, A. Shetty et al., High resolution gel-dosimetry by optical-CT and MR scanning. Med. Phys. **28**, 1436–1445 (2001). https://doi.org/10.1118/1.1380430
9. C. Baldock, P.J. Harris, A.R. Piercy et al., Experimental determination of the diffusion coefficient in two-dimensions in ferrous sulphate gels using the finite element method. Australas. Phys. Eng. Sci. Med. **24**, 19–30 (2001). https://doi.org/10.1007/BF03178282
10. P. Alexander, A. Charlesby, M. Ross, The degradation of solid polymethylmethacrylate by ionizing radiations. Proc. R. Soc. A **223**, 392–404 (1954). https://doi.org/10.1098/rspa.1954.0123
11. J.M. Joers, P.M. Fong, J.C. Gore, Detection of radiation effects in polymer gel dosimeters using 129Xe NMR. Phys. Med. Biol. **51**, N23–N30 (2006). https://doi.org/10.1088/0031-9155/51/2/N01
12. Y. Xu, C.S. Wuu, M.J. Maryanski, Performance of a commercial optical CT scanner and polymer gel dosimeters for 3-D dose verification. Med. Phys. **31**, 3024–3033 (2004). https://doi.org/10.1118/1.1803674
13. M. Hilts, C. Duzenli, Image filtering for improved dose resolution in CT polymer gel dosimetry. Med. Phys. **31**, 39–49 (2004). https://doi.org/10.1118/1.1633106
14. M.L. Mather, C. Baldock, Ultrasound tomography imaging of radiation dose distributions in polymer gel dosimeters: preliminary study. Med. Phys. **30**, 2140–2148 (2003). https://doi.org/10.1118/1.1590751
15. C. Baldock, L. Rintoul, S.F. Keevil et al., Fourier transform Raman spectroscopy of polyacrylamide gels (PAGs) for radiation dosimetry. Phys. Med. Biol. **43**, 17–27 (1998). https://doi.org/10.1088/0031-9155/43/12/017
16. J. Uusi-Simola, S. Savolainen, A. Kangasmäki et al., Study of the relative dose-response of BANG-3 polymer gel dosimeters in epithermal neutron irradiation. Phys. Med. Biol. **48**, 2895–2906 (2003). https://doi.org/10.1088/0031-9155/48/17/310
17. T.F. Mangueira, C.F. Silva, P.R. Coelho et al., Gamma/neutron dose evaluation using Fricke gel and alanine gel dosimeters to be applied in boron neutron capture therapy. Appl. Radiat. Isot. **68**, 791–794 (2010). https://doi.org/10.1016/j.apradiso.2010.01.027
18. P. Guo, J. Adamovics, M. Oldham, A practical three-dimensional dosimetry system for radiation therapy. Med. Phys. **33**, 3962–3972 (2006). https://doi.org/10.1118/1.2349686
19. J. Adamovics, M.J. Maryanski, Characterisation of PRESAGE: a new 3-D radiochromic solid polymer dosemeter for ionising radiation. Med. Phys. **120**, 107–112 (2006). https://doi.org/10.1093/rpd/nci555
20. T. Gorjiara, R. Hill, K. Kuncic et al., Investigation of radiological properties and water equivalency of PRESAGE® dosimeters. Med. Phys. **38**, 2265–2274 (2011). https://doi.org/10.1118/1.3561509
21. Z.S. Eznaveh, M.H. Zahamtkesh, A.R.K. Asl et al., Sensitivity optimization of PRESAGE polyurethane based dosimeter. Radiat. Meas. **45**, 89–91 (2010). https://doi.org/10.1016/j.radmeas.2009.08.005
22. S. Brown, A. Venning, Y. De Deene et al., Radiological properties of the PRESAGE and PAGAT polymer dosimeters. Appl. Radiat. Isot. **66**, 1970–1974 (2008). https://doi.org/10.1016/j.apradiso.2008.06.005
23. K. Jordan, N. Avvakumov, Radiochromic leuco dye micelle hydrogels: I. Initial investigation. Phys. Med. Biol. **54**, 141–153 (2009). https://doi.org/10.1088/0031-9155/54/22/002
24. S. Babic, J. Battista, K. Jordan, Radiochromic leuco dye micelle hydrogels: II. Low diffusion rate leuco crystal violet gel. Phys. Med. Biol. **54**, 6791–6808 (2009). https://doi.org/10.1088/0031-9155/54/22/003
25. J. Vandecasteele, S. Ghysel, S.H. Baete et al., Radio-physical properties of micelle leucodye 3D integrating gel dosimeters. Phys. Med. Biol. **56**, 627–651 (2011). https://doi.org/10.1088/0031-9155/56/3/007
26. T. Gorjiara, R. Hill, K. Kuncic et al., Water equivalence of micelle gels for X-ray beams. J. Phys.: Conf. Ser. **444**, 012024 (2013). https://doi.org/10.1088/1742-6596/444/1/012024
27. C. Baldock, R.F. Burford, N. Billingham et al., Experimental procedure for the manufacture and calibration of polyacrylamide gel (PAG) for magnetic resonance imaging (MRI) radiation dosimetry. Phys. Med. Biol. **43**, 695–702 (1998). https://doi.org/10.1088/0031-9155/43/3/019
28. M.J. Maryanski, R.J. Schulz, J.C. Gore, Three Dimensional Detection, Dosimetry and Imaging of an Energy Field by Formation of a Polymer in a Gel. US Patent 5,321,357 (1994)
29. A.R. Farajollahi, D.E. Bonnett, A.J. Ratcliffe et al., An investigation into the use of polymer gel dosimetry in low dose rate brachytherapy. Br. J. Radiol. **72**, 1085–1092 (1999). https://doi.org/10.1259/bjr.72.863.10700826

30. P. Sandilos, A. Angelopoulos, P. Baras et al., Dose verification in clinical IMRT prostate incidents. Int. J Radiat. Oncol. Biol. **59**, 1540–1547 (2004). https://doi.org/10.1016/j.ijrobp.2004.04.029
31. P. Kipouros, E. Pappas, P. Baras et al., Wide dynamic dose range of VIPAR polymer gel dosimetry. Phys. Med. Biol. **46**, 2143–2159 (2001). https://doi.org/10.1088/0031-9155/46/8/308
32. P.M. Fong, D.C. Keil, M.D. Does et al., Polymer gels for magnetic resonance imaging of radiation dose distributions at normal room atmosphere. Phys. Med. Biol. **46**, 3105–3113 (2001). https://doi.org/10.1088/0031-9155/46/12/303
33. Y. De Deene, C. Hurley, A. Venning et al., A basic study of some normoxic polymer gel dosimeters. Phys. Med. Biol. **47**, 3441–3463 (2002). https://doi.org/10.1088/0031-9155/47/19/301
34. H. Gustavsson, S. Back, M. Lepage et al., Development and optimization of a 2-hydroxyethylacrylate MRI polymer gel dosimeter. Phys. Med. Biol. **49**, 227–241 (2004). https://doi.org/10.1088/0031-9155/49/2/004
35. Y. De Deene, K. Vergote, C. Claeys et al., The fundamental radiation properties of normoxic polymer gel dosimeters: a comparison between a methacrylic acid based gel and acrylamide based gels. Phys. Med. Biol. **51**, 653–673 (2006). https://doi.org/10.1088/0031-9155/51/3/012
36. A. Venning, S. Brindha, B. Hill et al., Study of a normoxic PAG gel dosimeter with tetrakis (hydroxymethyl) phosphonium chloride as an anti-oxidant. J. Phys.: Conf. Ser. **3**, 155–158 (2004). https://doi.org/10.1088/1742-6596/3/1/016
37. R.J. Senden, P. De Jean, K. Mc, Auley, Schreiner L. Polymer gel dosimetry with reduced toxicity: a preliminary investigation of the NMR and optical dose-response using different monomers. Phys. Med. Biol. **51**, 3301–3314 (2006). https://doi.org/10.1088/0031-9155/51/14/001
38. I. Kantemiris, L. Petrokokkinos, A. Angelopoulos et al., Carbon beam dosimetry using VIP polymer gel and MRI. J. Phys.: Conf. Ser. **164**, 012055 (2009). https://doi.org/10.1088/1742-6596/164/1/012055
39. A.M. El-Khayatt, M.A. Al-Rajhi, Analysis of some lunar soil and rocks samples in terms of photon interaction and photon energy absorption. Adv. Space Res. **55**, 1816–1822 (2015). https://doi.org/10.1016/j.asr.2015.01.020
40. A.M. Ali, A.M. El-Khayatt, I. Akkurt, Determination of effective atomic number and electron density of heavy metal oxide glasses. Radiat. Eff. Defects Solids **171**(3–4), 202–213 (2016). https://doi.org/10.1080/10420150.2016.1170016
41. M. Kurudirek, S.V. Kurudirek, Collisional, radiative and total electron interaction in compound semiconductor detectors and solid state nuclear track detectors: effective atomic number and electron density. Appl. Radiat. Isot. **99**, 54–58 (2015). https://doi.org/10.1016/j.apradiso.2015.02.011
42. M. Kurudirek, Effective atomic numbers of different types of materials for proton interaction in the energy region 1 keV–10 GeV. Nucl. Instr. Methods Phys. Res. B **336**, 130–134 (2014). https://doi.org/10.1016/j.nimb.2014.07.008
43. M. Kurudirek, T. Onaran, Calculation of effective atomic number and electron density of essential biomolecules for electron, proton, alpha particle and multi-energetic photon interactions. Radiat. Phys. Chem. **112**, 125–138 (2015). https://doi.org/10.1016/j.radphyschem.2015.03.034
44. M. Kurudirek, Studies on heavy charged particle interaction, water equivalence and Monte Carlo simulation in some gel dosimeters, water, human tissues and water phantoms. Nucl. Instr. Methods Phys. Res. A **795**, 239–252 (2015). https://doi.org/10.1016/j.nima.2015.06.001
45. A. Brahme, Dosimetric precision requirements in radiation therapy. Acta Radiol. Oncol. **23**, 379–391 (1984). https://doi.org/10.3109/02841868409136037
46. P. Sellakumar, E.J.J. Samuel, S.S. Supe, Water equivalence of polymer gel dosimeters. Radiat. Phys. Chem. **76**, 1108–1115 (2007). https://doi.org/10.1016/j.radphyschem.2007.03.003
47. M.L. Taylor, R.D. Franich, J.V. Trapp et al., The effective atomic number of dosimetric gels. Australas. Phys. Eng. Sci. Med. **31**, 131–138 (2008). https://doi.org/10.1007/BF03178587
48. A. Un, Water and tissue equivalency of some gel dosimeters for photon energy absorption. Appl. Radiat. Isot. **82**, 258–263 (2013). https://doi.org/10.1016/j.apradiso.2013.09.002
49. E.P. Blizard, Nuclear radiation shielding. Annu. Rev. Nucl. Part. Sci. Annu. Rev. Nucl. Part. Sci. **5**, 73–98 (1955). https://doi.org/10.1146/annurev.ns.05.120155.000445
50. A.M. El-Khayatt, NXcom—a program for calculating attenuation coefficients of fast neutrons and gamma-rays. Ann. Nucl. Energy **38**, 128–132 (2011). https://doi.org/10.1016/j.anucene.2010.08.003
51. K.K. Shahri, L.R. Motavalli, H.M. Hakimabad, Neutrons applications in cancer treatment and in specific diagnostics. Hell J. Nucl. Med. **14**, 110–113 (2011) **(Editorial)**
52. M. Alqathami, A. Blencowe, M. Geso et al., Characterization of novel water-equivalent PRESAGE® dosimeters for megavoltage and kilovoltage x-ray beam dosimetry. Radiat. Meas. **74**, 12–19 (2015). https://doi.org/10.1016/j.radmeas.2015.02.002
53. ICRU Report No 44, *Tissue Substitutes in Radiation Dosimetry and Measurement* (International Commission of Radiation Units and Measurements, Bethesda, MD, 1989)
54. A.M. El-Khayatt, I. Akkurt, Photon interaction, energy absorption and neutron removal cross section of concrete including marble. Ann. Nucl. Energy **60**, 8–14 (2013). https://doi.org/10.1016/j.anucene.2013.04.021
55. S.R. Manohara, S.M. Hanagodimath, L. Gerward, Photon interaction and energy absorption in glass: a transparent gamma ray shield. J. Nucl. Mater. **393**, 465–472 (2009). https://doi.org/10.1016/j.jnucmat.2009.07.001
56. J.H. Hubbell, S.M. Seltzer, Tables of X-ray mass attenuation coefficients and mass energy-absorption coefficients 1 keV to 20 MeV for elements Z = 1 to 92 and 48 additional selected substances of dosimetric interest (1996), NISTIR-5632
57. M.F. Kaplan, *Concrete Radiation Shielding* (Wiley, New York, 1989)
58. J.H. Hubbell, Review of photon interaction cross section data in the medical and biological context. Phys. Med. Biol. **44**, R1–R22 (1999). https://doi.org/10.1088/0031-9155/44/1/001
59. J. Wood, *Computational Methods in Reactor Shielding* (Pergamon Press Inc, New York, 1982)
60. M. Alqathami, A. Blencowe, G. Qiao et al., Optimizing the sensitivity and radiological properties of the PRESAGE® dosimeter using metal compounds. Radiat. Phys. Chem. **81**, 1688–1695 (2012). https://doi.org/10.1016/j.radphyschem.2012.06.004
61. T. Gorjiar, R. Hill, S. Bosi et al., Water equivalence of NIPAM based polymer gel dosimeters with enhanced sensitivity for X-ray CT. Radiat. Phys. Chem. **91**, 60–69 (2013). https://doi.org/10.1016/j.radphyschem.2013.05.018